Journal of Catalysis 278 (2011) 321–328

Contents lists available at ScienceDirect

Journal of Catalysis

journal homepage: www.elsevier.com/locate/jcat

Effect of water on the adsorbed structure of formic acid on TiO_2 anatase (1 0 1)

Kristi L. Miller, John L. Falconer, J. Will Medlin *

Department of Chemical and Biological Engineering, University of Colorado, Boulder, CO 80309-0424, United States

ARTICLE INFO

Article history:
Received 26 August 2010
Revised 27 December 2010
Accepted 28 December 2010
Available online 2 February 2011

Keywords:
Photocatalysis
Formic acid
TiO_2
Water
Density functional theory (DFT)

ABSTRACT

The effect of water on the adsorption of formic acid on the anatase (1 0 1) surface of TiO_2 was investigated with density functional theory. These calculations showed that water co-adsorbed with formic acid promotes O–H bond dissociation to produce formate ions, but that the details of this chemistry depend on the surface coverage of formic acid. For 1/4 monolayer (ML) formic acid coverage, O–H dissociation required only a 1:1 ratio of water to formic acid. At 1 ML formic acid coverage, only 1/4 ML formic acid dissociated unless significant constraints were placed on water adsorption geometries. The density functional theory calculations also indicated that water converts bidentate bridging formate to monodentate formate. Comparisons with experimental data reveal that these transformations can have an important influence on elementary steps in the photocatalytic decomposition of formic acid on TiO_2 and Pt/TiO_2.

1. Introduction

Fundamental investigations into the surface chemistry of organic compounds on TiO_2 surfaces are of interest for a number of catalytic applications, including photocatalytic destruction of volatile organic compounds (VOCs). A number of previous studies have shown that water (present as a solvent or in a humid vapor phase) can have a profound influence on catalytic reactivity [1–7]. For example, we have recently shown that water co-dosed in the vapor phase can increase the rate of formic acid photocatalytic decomposition (PCD) on P25 TiO_2 by 25% and can increase the PCD rate by a factor of 8 on Pt/TiO_2 [8]. The more pronounced rate acceleration on Pt/TiO_2 was attributed to a change in the rate-determining step for formic acid PCD. Whereas the slow step on unpromoted TiO_2 was proposed to be abstraction of lattice oxygen for the water-forming reaction, the addition of Pt was found to provide a pathway for H_2 evolution so that the rate-determining step became the decomposition of formic acid adsorbed on TiO_2. Similarly, water has been found to have significant effects on the PCD or photocatalytic oxidation (PCO) of several other compounds on TiO_2; in some cases, water reduces catalyst activity through competitive adsorption with the reactant, while in other cases water accelerates the reaction through mechanisms that are not well understood [9–15]. Thus, fundamental investigations into the role of water in altering the surface chemistry of simple organic molecules, such as formic acid, on TiO_2 surfaces are of considerable interest.

In the present contribution, a systematic density functional theory (DFT) investigation of how water affects formic acid adsorption was conducted by examining different coverages of water and formic acid. The behavior of co-adsorbed formic acid and water depends on their relative coverages. Secondary interactions, such as hydrogen bonding with both the surface and co-adsorbed species, influence the adsorption mode of a molecule on a metal oxide [16]. Vittadini et al. [17] used DFT to determine that water adsorbs dissociatively at 1/4 monolayer (ML) on anatase (0 0 1). At water coverages of 1 ML and higher, molecular water is also present because all the surface titanium sites are filled with hydroxyls. The hydroxyls are either from water that dissociated on a surface titanium or from hydrogen adsorption on the surface oxygen; this breaks the bond between the surface oxygen and titanium atoms and creates a hydroxyl bound to the adjacent titanium atom. The molecularly adsorbed water forms two hydrogen bonds, one with a hydroxyl and the other with a surface oxygen. Using DFT, Gong et al. [18] obtained different formate geometries depending on water coverage on anatase (0 0 1). At 1/2 ML water coverage, formic acid physisorbs because hydroxyls fill all surface Ti sites. At 1/6 ML water coverage, formic acid adsorbs as bidentate bridging formate, and at 1/3 ML water coverage, formic acid adsorbs as bidentate chelating formate due to site competition. Fig. 1 illustrates the formate structures of bidentate bridging (BB), bidentate chelating (B), and monodentate (M).

For the work reported here, DFT was used to determine the effect of co-adsorbed water on adsorbed formic acid at different water and formic acid coverages on anatase (1 0 1) and in selected cases on rutile (1 1 0); these are the most stable anatase and rutile surfaces [18]. Comparisons are made to experimental

---

* Corresponding author. Fax: +303 492 4341.
E-mail address: will.medlin@colorado.edu (J.W. Medlin).

0021-9517/$ - see front matter © 2010 Elsevier Inc. All rights reserved.
doi:10.1016/j.jcat.2010.12.019

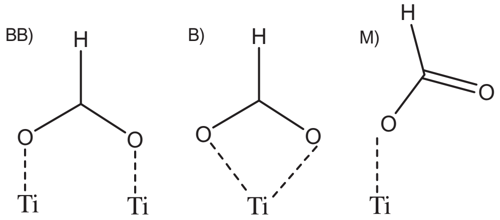

Fig. 1. Formate adsorption geometries. BB is bidentate bridging, B is bidentate chelating, and M is monodentate.

investigations into the same chemistry, with frequency calculations used to facilitate interpretation of previously reported infrared spectra.

2. Methods

The Vienna Ab initio Simulation Package (VASP) was used for DFT calculations [19,20]. A repeated slab geometry modeled the TiO_2 surface, with two anatase (1 0 1) slab sizes and a rutile (1 1 0) slab used in calculations. The large anatase slab consisted of a 2 × 2 unit cell, 2 layers thick, and contained $16TiO_2$ units with the anatase (1 0 1) surface exposed. The slab dimensions were 1.02, 0.76, and 0.60 nm in the *x*, *y*, and *z* directions, respectively. The small slab contained $4TiO_2$ units with the (1 0 1) surface exposed, and its dimensions were 0.51, 0.38, and 0.60 nm in the *x*, *y*, and *z* directions, respectively. Both slabs were separated by a vacuum of 2 nm. The rutile slab consisted of a unit cell three layers thick and contained 16 titanium atoms and 32 oxygen atoms. The slab dimensions were 0.65, 0.59, and 1.26 nm in the *x*, *y*, and *z* directions. The rutile slab was separated by a vacuum of 3.0 nm. Ultrasoft pseudopotentials described electron-core interactions for Ti and O [21]. The generalized gradient approximation (GGA) was implemented using the PW91 potential. Molecules were adsorbed on the relaxed upper surface of the slab, and the slab's lower half remained fixed. All calculations used a cutoff energy of 33 MJ/mol (25 Rydbergs) and a 5 × 5 × 5 Monkhort–Pack *k*-points mesh. Adsorption energies, equilibrium structures, and vibrational frequencies were calculated for adsorbed water, formic acid, and formate. Subtracting the energies of the relaxed bare slab and the gas-phase molecule from the energy of the adsorbate-covered slab results in a computed molecular adsorption energy:

$$E_{organic\ ads} = E_{organic+Slab} - E_{Slab} - E_{organic}$$

A new energy for the hydrated slab was calculated for all water coverages. To calculate the adsorption energy for formate, an H atom was removed from formic acid and adsorbed on the 2c-O of the slab. The energies of the hydrated surface and the gas-phase molecule were subtracted from the energy of the hydrated, adsorbate-covered slab:

$$E_{organic\ ads} = E_{Hydrated\ organic+Slab} - E_{Hydrated\ Slab} - E_{organic}$$

The starting configurations for formic acid, formate, and water were determined by examining previous studies, approximating where bonding may occur, and varying adsorption geometries to increase the probability of detecting the lowest energy structures.

3. Results and discussion

3.1. Formic acid adsorption

In agreement with previous literature, DFT calculations indicated that molecular adsorption of formic acid was thermodynamically favored over dissociative adsorption on anatase (1 0 1) [16]. Calculations used the *trans* formic acid configuration, which is more stable than the *cis* configuration [16,22]. The adsorption energy of molecular formic acid was computed to be −91 kJ/mol at 1/4 ML coverage. Monodentate and bidentate formate at 1/4 ML coverage were less stable, with adsorption energies of −20 and −48 kJ/mol, respectively. This agrees with the results of Vittadini et al., who modeled formic acid at 1/4 coverage on anatase (1 0 1) [16]. In our calculations, monodentate formate spontaneously produced formic acid when optimized close to a co-adsorbed H atom. Thus, the H had to be placed at a remote location on the slab for formate calculations to converge. The bidentate chelating structure was found to be unstable and converged to monodentate formate. Coordinatively unsaturated ions, 5c-Ti and 2c-O, and fully coordinated ions, 6c-Ti and 3c-O, make up the anatase (1 0 1) surface. Adsorption occurs on the more reactive 5c-Ti and 2c-O sites [16]. Formic acid molecularly adsorbed through the carbonyl oxygen (Lewis base) to a surface 5c-Ti (Lewis acid). Formic acid may preferentially bond through the carbonyl group because the carbonyl is a stronger Lewis base than the hydroxyl group. Hydrogen bonding between the hydroxyl proton and 2c-O also played an important role in stabilizing this structure. Fig. 2 illustrates adsorption structures for formic acid (2a) and monodentate (2b) and bidentate (2c) formate, and formic acid dimer (2d), and Table 2 summarizes adsorption energies.

The optimized geometry and adsorption energy of adsorbed formic acid did not depend on coverage from 1/4 to 1 ML (i.e., on the 2 × 2 and 1 × 1 unit cells) due to a lack of interaction between the adsorbed molecules. (Please see Supporting Fig. S1 for an image showing the relative positions of formic acid molecules adsorbed in adjacent unit cells.) This result suggests that formic acid can accumulate to high coverages on anatase (1 0 1), as observed

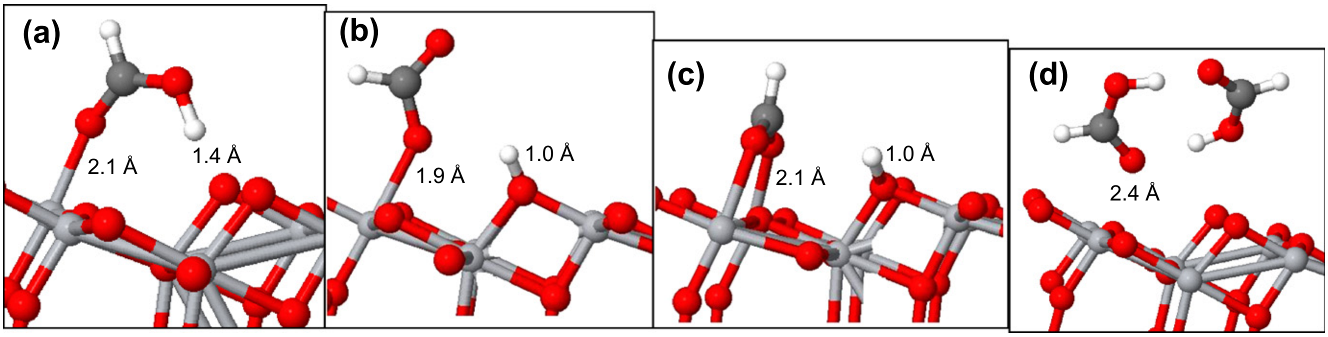

Fig. 2. DFT-optimized geometries of (a) molecular formic acid (adsorption energy *E* = −91 kJ/mol), (b) monodentate formate (*E* = −20 kJ/mol), (c) bidentate bridging formate (*E* = −48 kJ/mol), (d) formic acid dimer (*E* = −59 kJ/mol) adsorbed on TiO_2 anatase (1 0 1) at 1/4 ML coverage. Light gray and black (red) represent Ti and O atoms for the slab. For formic acid, dark gray represents C, black (red) is oxygen, and white is hydrogen. (For interpretation of the references to colour in this figure legend, the reader is referred to the web version of this article.)

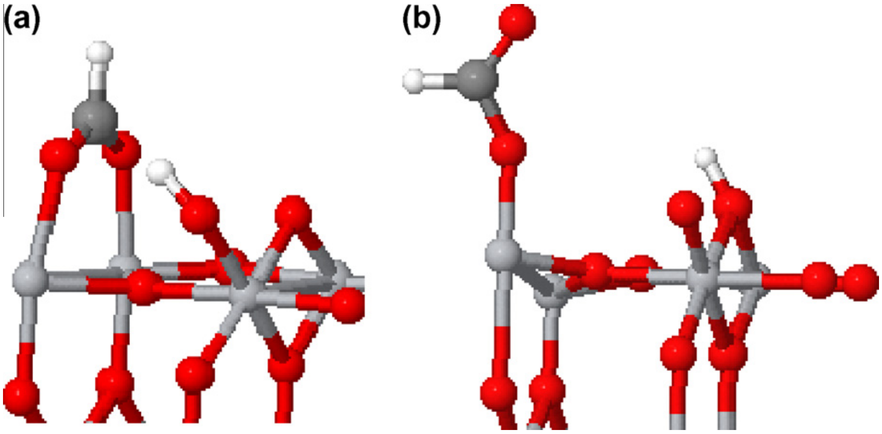

Fig. 3. DFT-optimized geometries of (a) bidentate bridging formate (adsorption energy $E = -102$ kJ/mol), (b) monodentate formate ($E = -30$ kJ/mol) adsorbed on TiO_2 rutile (1 1 0) at 1/4 ML coverage. Light gray and black (red) represent Ti and O atoms for the slab. For formic acid, dark gray represents C, black (red) is oxygen, and white is hydrogen. (For interpretation of the references to colour in this figure legend, the reader is referred to the web version of this article.)

Table 1
Vibration frequencies from FTIR and VASP of formic acid molecularly and dissociatively adsorbed on TiO_2.

Assignments	IR on P25 TiO_2 [8]		DFT			
	HCOOH	HCOOH and H_2O	Formic acid	Monodentate formate	Bidentate formate	Monodentate formate w/H_2O
COO and CH formate	2945	2945				
CH formic acid	2921	2921	3012			
CH formate	2867	2861		2900	2935	2882
C=O p-formic acid	1787					
c-formic	1675		1651			
COO— asym, MM formate		1565		1504		1696
COO— asym, BB formate	1550	1550			1494	
COO— sym, BB formate	1378	1378			1327	
COO— sym, M formate	1360	1360		1342		1157
CH formate	1323	1323		1359	1363	1340
CO or CH c-formic acid	1263		1352			
CO or CH p-formic acid	1105		1259			

c denotes chemisorbed and p denotes physisorbed.

experimentally. For example, experimental studies have shown that 4×10^{14} molecules/cm^2 are adsorbed on P25 TiO_2.[8] Formic acid at 1 ML coverage on anatase (1 0 1) corresponds to a coverage of 5×10^{14} molecules/cm^2. The adsorption energy was −91 kJ/mol at 1/4 ML coverage and −92 kJ/mol at 1 ML coverage. Adsorption of formic acid in a dimer form was less stable, with an adsorption energy of −59 kJ/mol.

Exploratory DFT calculations were also made on the rutile (1 1 0) surface to determine whether the trends observed for formate adsorption on anatase (1 0 1) may be more general, as discussed in further detail in the following sections. Bidentate formate (adsorption energy of −102 kJ/mol) is more stable than monodentate formate (−30 kJ/mol) on the rutile (1 1 0) surface (Fig. 3a and b). This agrees with findings by Rotzinger et al. [23] that formate adsorbs on rutile (1 1 0) TiO_2 as bidentate formate.

DFT frequency calculations were made for molecular formic acid and for bidentate and monodentate formate at 1/4 ML coverage for comparison with formate adsorption peaks in the IR spectra. These calculations were made on the anatase (1 0 1) surface, although formate likely forms on defect sites or other surfaces, as discussed above. The chelating geometry is less stable than the other two formate forms, so this configuration was not examined. Table 1 summarizes the results of these calculations and compares them with recently published IR spectra collected after adsorption of formic acid on P25 TiO_2. The CH or OH stretching frequencies from formic acid and formate averaged 6 ± 3% higher than the IR values. The calculated C=O and COO— frequencies averaged 3 ± 1% lower than IR values. Vibrations with hydrogen bonding modes have been shown to cause greater errors in DFT frequency calculations because DFT generally overestimates the hydrogen bond strength [24]. The DFT calculations treat hydrogen as a classical particle as opposed to a quantum particle; this decreases the average bond length [25,26]. The bond energy overestimation causes an IR frequency overestimation.

Because of this systematic error, differences in vibrational frequencies were used for comparison. Previous researchers have tracked the difference between the asymmetric and symmetric COO stretching modes ($\Delta\nu_{as-s}$) of formate to distinguish between monodentate and bidentate formate [27,28]. The value of $\Delta\nu_{as-s}$ for bidentate formate was 167 cm^{-1}, which is comparable to the IR result of 172 cm^{-1}. The $\Delta\nu_{as-s}$ for monodentate formate was 356 cm^{-1}. This helps confirm that bidentate formate is on the P25 surface. However, we note that the predominant adsorption mode for formic acid on P25 TiO_2 was found to be the intact molecule, in line with our calculations here that formic acid adsorption is more stable than either formate binding mode. As shown below, the presence of water can change this preference.

3.2. Effect of water on formic acid adsorption

Density functional theory calculations indicated that the relative stabilities of formic acid and the various formate configurations on anatase (1 0 1) depended strongly on the relative coverages of water and formic acid. Water adsorbs molecularly on the anatase (1 0 1) 5c-Ti sites in a chemisorbed state with an adsorption energy of −65 kJ/mol. Previous STM and XPS studies [29,30] and DFT calculations [17,31] also show molecular (non-dissociative) adsorption of water, and the adsorption energy computed here agrees with previous DFT calculations [17,31]. As discussed below, additional water beyond that necessary to complete the monolayer results in the formation of additional, physisorbed layers. In the simulations of the effect of water reported here, we initiated calculations with the relatively well-defined structure of water adsorbed in its monolayer state. For coverages exceeding one monolayer, we then sequentially added water molecules (with intermediate geometry optimization) for each higher coverage calculation. It is noted that such an approach does not simulate a solution phase, but rather allows one to explore the effect of hydrogen bond formation on stabilization of intermediates.

Initial calculations aimed at identifying the likely effect of water considered a minimal 12-atom slab. Such a system has the restriction that the formic acid and water coverages are each one monolayer at minimum. More problematically, the minimal unit cell requires that each formic acid molecule, as well as each water molecule in a given layer, adopts the same orientation. This is a major simplification of the true case, where water molecules can take on a variety of orientations around adsorbed formic acid. Nevertheless, consideration of the minimal unit cell provides a simple platform for insights into how H-bonding interactions between water and formic acid can alter formic acid adsorption. Below, we discuss more complex models of the interface.

Calculations with the minimal 12-atom slab showed that a second water layer was needed to dissociate formic acid at 1 ML coverage. With one water monolayer, the adsorption energy of molecular formic acid was −77 kJ/mol, which is higher than the −58 kJ/mol for dissociated formic acid, indicating that molecular adsorption was favored. As shown in Fig. 4a, water preferentially adsorbed on the 5c-Ti site and formic acid molecularly adsorbed through the hydroxyl group hydrogen to the surface 2c-O. The carbonyl oxygen atom bonded to a hydrogen atom from water. When formic acid was placed on 5c-Ti sites (the preferred sites in the absence of water) with water adsorbed through hydrogen interactions with surface oxygens, it remained molecularly adsorbed with weaker adsorption energy of −57 kJ/mol (Fig. 4b).

In contrast, a second water layer promoted formic acid dissociation due to stabilization through hydrogen bonding. Multiple starting conditions, including formic acid molecularly and dissociatively adsorbed with water only in the 2nd layer and water adsorbed on the 5c-Ti sites and in the 2nd layer, were employed to ensure that the most favorable configuration was determined. In all cases, one water adsorbed on the 5c-Ti site and the second water remained in the 2nd layer. Water blocked the 5c-Ti atom used for formic acid adsorption through the carbonyl oxygen and created the need for additional stabilization. With two water layers, the adsorption energy of formate was −63 kJ/mol, and thus, it was significantly more stable than molecular formic acid with an adsorption energy of −20 kJ/mol. The two configurations are shown in Fig. 5. Two water layers induced dissociation because the second water layer stabilized formate by forming hydrogen bonds with the oxygen atoms from the hydroxyl and carbonyl. The addition of the second water layer also caused the first water layer to dissociate to a hydroxyl and a hydrogen. Because the formation of surface hydroxyls appears to be key for this chemistry, the effect of adsorbed hydroxyls on formic acid adsorption was also examined. When 1 ML formic acid was co-adsorbed with a hydroxyl, molecular formic acid was favored with an adsorption energy of −73 kJ/mol. One ML of formate co-adsorbed with an hydroxyl was unstable with a adsorption energy of 61 kJ/mol. This confirmed that formic acid dissociation required hydrogen bond stabilization, and not simply a hydroxyl group.

The calculations described above suggest that water can have a profound effect on the adsorption and dissociation of formic acid at sufficient coverage; however, as described below, the effect of the small unit cell used for these initial calculations is significant, as was shown by conducting calculations on a larger unit cell. When 3/4 ML of water was added to a surface that had 1/4 ML formic acid, the adsorption energy of formic acid decreased from −91 to −77 kJ/mol. Water also decreased the formic acid dimer's stability from −59 to −46 kJ/mol for each formic acid molecule. Although water destabilized formic acid, it increased the stability of mono-

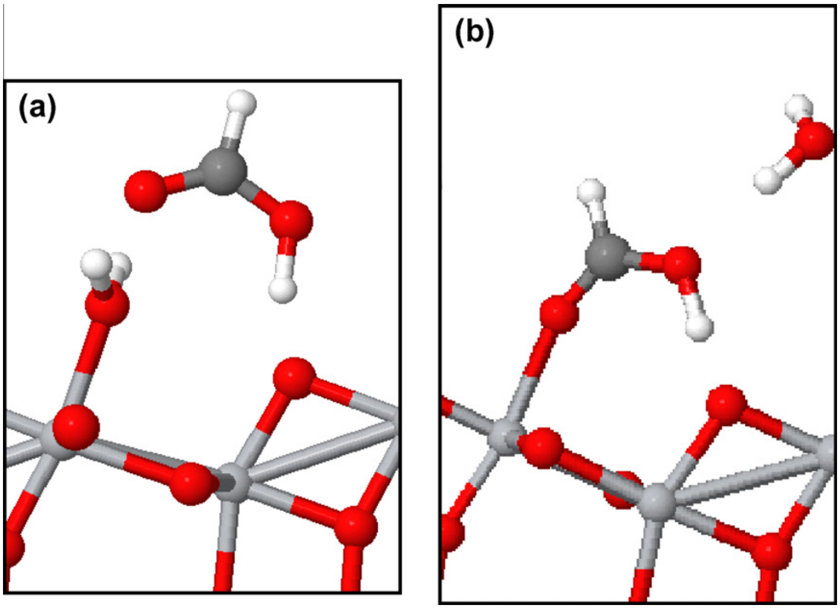

Fig. 4. DFT-optimized configurations of (a) chemisorbed water with 1 ML formic acid (adsorption energy $E = -77$ kJ/mol) and (b) physisorbed water with 1 ML formic acid ($E = -57$ kJ/mol) on anatase (1 0 1). Light gray and black (red) represent Ti and O atoms for the slab. For formic acid, dark gray represents C, black (red) is oxygen, and white is hydrogen. (For interpretation of the references to colour in this figure legend, the reader is referred to the web version of this article.)

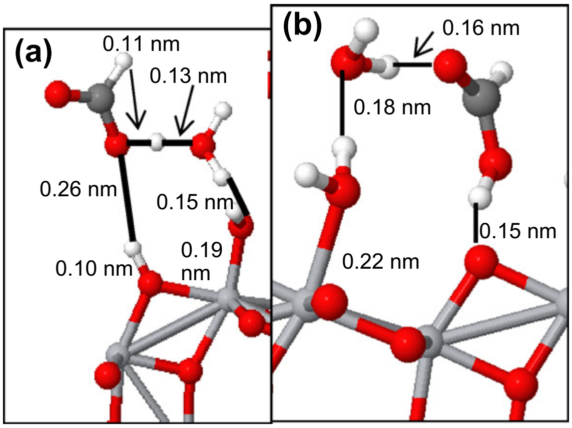

Fig. 5. DFT-optimized configurations of (a) 1 ML formate with 2 water layers (adsorption energy $E = -63$ kJ/mol), (b) 1 ML molecular formic acid with 2 water layers (−20 kJ/mol) on anatase (1 0 1). Light gray and black (red) represent Ti and O atoms for the slab. For formic acid, dark gray represents C, black (red) is oxygen, and white is hydrogen. (For interpretation of the references to colour in this figure legend, the reader is referred to the web version of this article.)

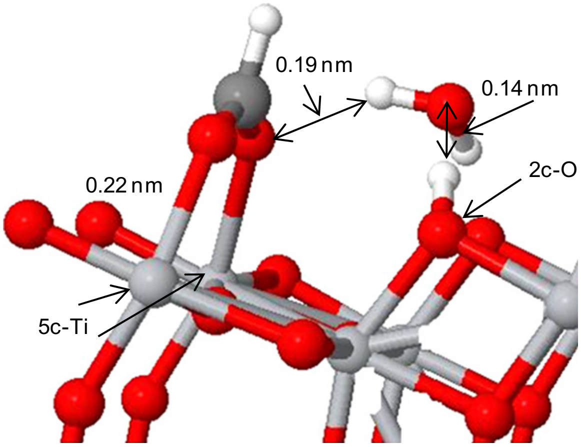

Fig. 7. DFT-optimized configuration of 1/4 ML bidentate formate co-adsorbed with 1/4 ML water (adsorption energy $E = -48$ kJ/mol) on anatase (1 0 1). Light gray and black (red) represent Ti and O atoms for the slab. For formic acid, dark gray represents C, black (red) is oxygen, and white is hydrogen. (For interpretation of the references to colour in this figure legend, the reader is referred to the web version of this article.)

Table 2
Adsorption energies of formic acid with and without water on anatase (1 0 1).

HCOOH coverage (ML)	Water coverage (ML)	Unit cell size	Adsorption energy[a] (kJ/mol)	Type of adsorption	Figure #
1	0	1 × 1	−92	Molecular	
1/4	0	2 × 2	−91	Molecular	2a
1/4	0	2 × 2	−20	M formate	2b
1/4	0	2 × 2	−48	BB formate	2c
½	0	2 × 2	−59	Dimer	2d
1	1	1 × 1	−58	Dissociative	
1	1	1 × 1	−77	Molecular	4
1	2	1 × 1	−63	Dissociative	5a
1	2	1 × 1	−20	Molecular	5b
1/4	¾	2 × 2	−77	Molecular	
1/4	¾	2 × 2	−86	M formate	6[b]
1/4	¾	2 × 2	−48	BB formate	7[b]
½	¾	2 × 2	−46	Dimer	
1	1	2 × 2	−41	1/4 ML formate, 3/4 ML molecular	S2
1	2	2 × 2		1/4 ML formate, 3/4 ML molecular	

[a] Adsorption energies are for formic acid and formate with the dissociated hydrogen included.

[b] Figures are shown using 1/4 ML water for clarity.

dentate formate from −20 to −86 kJ/mol. The dissociated state became more stable than the molecular state because hydrogen bonding stabilized the formate structure. Water and the hydrogen on 2c-O formed hydrogen bonds with the oxygen of formate at distances of 0.18 and 0.14 nm (Fig. 6). The bidentate formate adsorption energy of −48 kJ/mol did not change with water addition because both formate oxygen atoms bonded to surface 5c-Ti atoms (Fig. 7). The bidentate chelating structure was not stable with water addition and became monodentate formate with one oxygen bonded to 5c-Ti at a distance of 0.20 nm compared with 0.21 nm without water. The adsorption energies are summarized in Table 2.

As an exploratory probe of how varying surface structures alter the effect of water on formic acid adsorption and dissociation, similar calculations were made on rutile (1 1 0). Water also increased the adsorption energy of monodentate formate from −30 to −58 kJ/mol. Water stabilized monodentate formate on rutile in the same way as on anatase (1 0 1), with hydrogen bonding between the hydrogen from water to the formate oxygen (Fig. 8). Gong et al. [18] studied co-adsorption of water and formic acid on anatase (0 0 1). Water was found not to stabilize monodentate on the unreconstructed surface, apparently because the formate oxygen is already hydrogen bonded with the H on the 2c-O without water present. Also, anatase (0 0 1) reconstructs under UHV conductions, with the surface energy for the reconstructed surface half that of the unreconstructed structure. Monodentate formate was stabilized on the surface ridges of the reconstructed surface where a hydrogen bond (0.16 nm) formed between the 2c-O–H and oxygen of formate, which was binding to 4c-Ti, and monodentate formate was observed on the surface ridges from STM images. Thus, an overall picture emerges that a surface capable of extensive hydrogen bonding results in preferential stabilization of monodentate formate over bidentate formate.

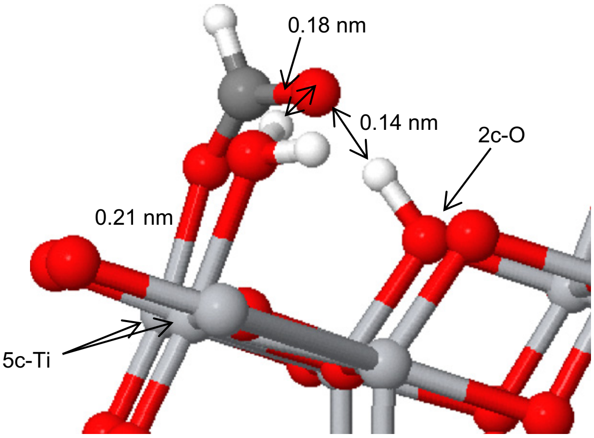

Fig. 6. DFT-optimized geometry of 1/4 ML monodentate formate co-adsorbed with 1/4 ML water (adsorption energy $E = -86$ kJ/mol) on anatase (1 0 1). Light gray and black (red) represent Ti and O atoms for the slab. For formic acid, dark gray represents C, black (red) is oxygen, and white is hydrogen. (For interpretation of the references to colour in this figure legend, the reader is referred to the web version of this article.)

The water coverage was varied from 1/4 to 2 ML to determine how water coverage affects the dissociation of 1/4 ML formic acid on anatase (1 0 1). Formic acid molecularly adsorbed on the 5c-Ti on a 48-atom unit cell, and water coverage was varied by adsorbing water molecules sequentially (with geometry optimizations after addition of each water molecule) on the three remaining

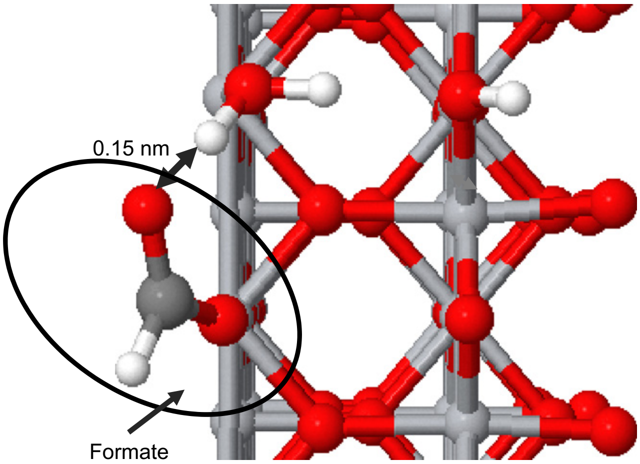

Fig. 8. DFT-optimized geometry of 1/4 ML monodentate formate co-adsorbed with 1/4 ML water (adsorption energy $E = -58$ kJ/mol) on rutile (1 1 0). Light gray and black (red) represent Ti and O atoms for the slab. For formate, dark gray represents C, black (red) is oxygen, and white is hydrogen. (For interpretation of the references to colour in this figure legend, the reader is referred to the web version of this article.)

5c-Ti sites and then placing additional water molecules above the first layer until a total of 8 water molecules were adsorbed. Formic acid dissociated to produce monodentate formate at all water coverages with the hydroxyl hydrogen transferring to the 2c-O site to form a 0.11-nm O–H bond. The carbonyl oxygen remained bonded to the 5c-Ti atom at a distance of 0.21 nm, and water formed hydrogen bonds with the hydroxyl oxygen at a distance of 0.18 nm (Fig. 7). Due to the strength of the carbonyl oxygen bond to the 5c-Ti atom, hydroxyl dissociation required stabilization by hydrogen bonding. Formic acid dissociated with all water coverages, but the bond distance between oxygen and hydrogen increased by 0.01 nm as water coverage was increased above 1 ML (i.e., with increased solvation). All other changes in adsorption structures were minimal, and adsorption energies were relatively uniform with a slightly decreasing trend (from −89 kJ/mol at 1/4 ML water coverage to −80 kJ/mol at 2 ML coverage). At all water coverages, dissociation of 1/4 ML formic acid to formate was preferred.

To investigate whether water promoted dissociation of higher coverages of formic acid on a larger, more realistic unit cell, water coverages were varied from 1 to 2 ML on a 48-atom slab onto which one monolayer of formic acid was preadsorbed. In contrast to the calculations reported above for a minimal 12-atoms slab, the 48-atom slab (a 2 × 2 unit cell) allowed the four formic acid molecules and four water molecules per layer in the unit cell to take on different geometries. Initial geometries were varied by starting with either formate or molecular formic acid adsorbed and changing bonding positions. Mixed molecular and dissociative formic acid adsorption was seen on the 48-atom slab at 1 ML formic acid and 1 ML water coverage. In the most stable adsorbed configuration, one monodentate formate bonded to 5c-Ti and the remaining three formic acids adsorbed molecularly to a 2c-O through the hydroxyl group hydrogen as shown in Fig. S2 in the Supporting information. Three waters adsorbed on the 5c-Ti sites, and the remaining water remained in the second layer. Hydrogen bonding between water and the carboxyl oxygen (distances of 0.16 nm to 0.19 nm between molecules) stabilized the molecularly adsorbed formic acids. These results suggest that the extent of formic acid decomposition may be limited at high coverage with 1 ML of water present. When two of the formic acid molecules were dissociated as a starting configuration, they remained dissociated but the adsorption energy was −20 kJ/mol compared to −41 kJ/mol for one dissociated and three molecular formic acid molecules. When all four formic acid molecules were molecularly adsorbed, they remained molecularly adsorbed, and the adsorption energy was only slightly lower at −39 kJ/mol, suggesting a very weak propensity for dissociation of a single formic acid. (Note that the adsorption energies are lower in magnitude on the more crowded surface in the presence of water, in contrast to observations in the absence of water, where repulsive effects between adsorbed formic acid molecules were not observed.) Calculations made with up to two monolayers of adsorbed water showed an identical trend, in which dissociation of only 1/4 ML of formic acid was favorable, with a slightly reduced adsorption strength of −30 kJ/mol. Thus, the additional degrees of freedom afforded by the 2 × 2 unit cell, with four discrete formic acid molecules and the corresponding water, reveal that extensive formic acid dissociation is not favorable at high coverages and that removal of much of the formic acid is likely required to isolate formate on the surface. This point is discussed in more detail below.

In summary, DFT calculations on a 2 × 2 unit cell indicate that at 1/4 ML, formic acid dissociates even with a submonolayer of co-adsorbed water, whereas dissociation of higher coverages of formic acid is much less favorable, with 1/4 ML at maximum dissociating on the fully covered surface. Only in the case of a highly constrained 1 × 1 unit cell does a second water layer induce formic acid dissociation at 1 ML coverage by creating extensive hydrogen bonding between water and formic acid. To observe more extensive decomposition of formic acid to formate at high coverages, some of the formic acid likely needs to be removed, either through displacement or through photocatalytic reaction.

These DFT results predict that low coverages of formic acid will dissociate with water addition, but additional stable adsorbed formate was not observed after water addition to formic acid-covered P25 TiO_2 in experimental studies [8]. During IR measurements, water displaced nearly all the formic acid from the TiO_2 surface so that formate (presumably adsorbed on defect sites or other surface planes) was the primary species remaining. This is commonly seen with water addition to an organic-covered surface, even if the organic forms stronger bonds to the surface than water. Muggli et al. [32] showed that water displaces formic acid, and Backes et al. [33] showed that water displaces acetic acid on P25 TiO_2. Henderson et al. [1,34] determined that water displaces acetone on rutile TiO_2 due to dipole/dipole repulsions between adsorbed acetone molecules. The DFT calculations indicated that formic acid has a relatively weak adsorption energy of −91 kJ/mol, which (based on experimental results) is evidently not sufficiently strong to allow retention during water exposure. Any additional formate formed by water with an adsorption energy of lower than −91 kJ/mol would also likely be displaced by water and not detected experimentally. It should be noted that though commonly observed, the mechanism for water displacement of more strongly adsorbed organics from TiO_2 surfaces is not clear. However, some discussion of this somewhat counterintuitive result is warranted. Under the conditions of the previously reported experimental studies, adsorbed formic acid was in a kinetically rather than thermodynamically stable state, since the measurements were taken after removing formic acid from the vapor phase. Assuming a pre-exponential factor for desorption of $10^{13}\ s^{-1}$, the computed reduction in adsorption energy of formic acid (from −91 to −77 kJ/mol for a surface covered by 1/4 ML formic acid and 3/4 ML added water) is equivalent to an ~300-fold decrease in the half-life of adsorbed formic acid at room temperature. Furthermore, the half-life after water addition is computed to be on the order of seconds. Although these assumptions do not allow for quantitative prediction, clearly the computed change in adsorption energies could be consistent with the rapid decrease in the amount of adsorbed formic acid after water addition over the time scale of the reported measurements. On other surface planes, however, formic acid or formate appears to be more strongly adsorbed. Adsorption energies for bidentate formate were calculated by Gong et al. [18] to be −151 kJ/mol on anatase (0 0 1) and by McGill et al. [35] to be −153 kJ/mol on rutile (0 1 1). These significantly stronger adsorption energies suggest that formate adsorbed on less abundant surfaces may have a higher kinetic barrier for displacement by water.

On the other hand, stabilization of monodentate relative to bidentate formate by water adsorption, as predicted by DFT, may be consistent with the previous experimental studies on P25 TiO_2 measurements that showed a shift in the positions of the symmetric and asymmetric COO— stretching modes after adsorption of water [8]. Comparisons are complicated by the fact that the remaining formate is likely to be adsorbed on surfaces other than anatase (1 0 1); however, the exploratory calculations on other surfaces presented above indicate that the trend of monodentate stabilization through hydrogen bonding with water may be a general one. The Δv_{as-s} for COO— was calculated to be much larger for monodentate (356 cm^{-1}) than for bidentate (167 cm^{-1}) formate in the absence of water, and FTIR with water added showed a Δv_{as-s} of 205 cm^{-1} (Table 3). To explore the formate COO— frequency shift seen with IR, vibrational frequencies were calculated for monodentate and bidentate formate on a 2 × 2 unit cell with three co-adsorbed water molecules. The addition of co-adsorbed water caused a dramatic shift in the monodentate formate Δv_{as-s} value, from 356 cm^{-1} without water (peaks at 1696 and 1157 cm^{-1}) to 162 cm^{-1} with three waters (peaks at 1504 and 1342 cm^{-1}). Water stabilized the structure by forming hydrogen bonds with the formate oxygen, and this likely caused the decrease in Δv_{as-s}. Thus, a water-induced transition from bidentate to monodentate formate would not be expected to be accompanied by a large shift in the Δv_{as-s} value, consistent with experimental results, because the Δv_{as-s} value calculated from DFT for monodentate with water is similar to bidentate formate. However, because of the similar Δv_{as-s} values computed for monodentate and bidentate formate, the limited accuracy of these calculations [25,26], and the difference in substrates (anatase(1 0 1) versus P25 TiO_2), it is not possible to conclusively ascribe the experimentally observed frequency shifts as being due to a conversion of bidentate to monodentate formate; rather, it is simply noted that such a conversion (suggested by the DFT calculations) is not inconsistent with the experimental data.

3.3. Implications for photocatalysis

The calculations reported here have primarily been made on the anatase (1 0 1) surface, along with some exploratory results for rutile (1 1 0). Much of the experimental work probing the effects of water on photocatalytic rates has been conducted on high surface area materials (in particular P25 TiO_2) with numerous exposed crystal planes and even multiple crystalline phases. Thus, one must use extreme caution in making precise links between experimental measurements on high surface area materials and the single crystal results reported here. Nevertheless, these DFT calculations indicate general trends that may be important in the promotion of formic acid photodecomposition over TiO_2.

Table 3
COO— Δv_{as-s} from DFT on anatase (1 0) and experimental IR on P25 TiO_2.

Adsorption	DFT Δv_{as} (cm^{-1})	IR Δv_{as-s} (cm^{-1}) on P25 TiO_2 [8]
Bidentate	167	172
Monodentate	356	N/A
Monodentate with water	162	205

One effect of water is to stabilize monodentate formate relative to adsorbed formic acid, potentially promoting the dissociation reaction:

$$HCOOH(s) \rightarrow HCOO(s) + H(s)$$

This reaction is typically invoked as the initial bond-breaking step in formic acid PCD [36–38]. Thus, water may increase the rate of this step through the formation of favorable hydrogen bonding interactions with the product of this step, formate. Additionally, water appears to stabilize monodentate formate relative to bidentate formate on the surface by providing stabilizing hydrogen bonding interactions that allow bidentate formate to break one of its interactions with the surface. Previous investigations have indicated that the decomposition of formate occurs more rapidly for monodentate formate than for bidentate formate [39,40]. Thus, water may accelerate the rates of key elementary steps in formic acid decomposition in at least two ways. In addition, the co-adsorption of water and formic acid causes the formation of hydroxyl species on the surface, which can themselves serve as strong oxidizing agents in the photocatalytic reactions.

Finally, it is noted that the results reported here indicate a strong dependence of the effect of water on the coverage of both water and formic acid. While making direct comparisons between the limiting cases probed in this work and experimental measurements on high surface area TiO_2 is difficult, these results may suggest that a limited coverage of formic acid is convertible to formate through promotion by water, perhaps accounting for the substantial desorption (rather than total decomposition) of formic acid after water adsorption.

4. Conclusions

Density functional theory (DFT) calculations indicated that formic acid adsorbed molecularly on a dry anatase (1 0 1) surface, but dissociated to monodentate formate when water adsorbed, depending on formic acid and water coverages. At 1 ML formic acid coverage, dissociation required 2 ML of water, but as at 1/4 ML formic acid coverage, dissociation required only 1/4 ML of water. Adsorption of water also resulted in a change in the most stable adsorption geometry of formate from bidentate to monodentate. These changes in the adsorbed structure of formic acid and formate may relate to experimentally observed increases in PCD rate after addition of water.

Acknowledgment

We gratefully acknowledge support by the National Science Foundation, Grant CBET0730047.

Appendix A. Supplementary material

Supplementary data associated with this article can be found, in the online version, at doi:10.1016/j.jcat.2010.12.019.

References

[1] M.A. Henderson, J. Catal. 256 (2008) 287.
[2] L.F. Liao, C.F. Lien, D.L. Shieh, M.T. Chen, J.L. Lin, J. Phys. Chem. B 106 (2002) 11240.
[3] S. Sato, JCS – Chem. Commun. (1982) 26.
[4] S. Sato, J. Phys. Chem. 87 (1983) 3531.
[5] M. El-Maazawi, A.N. Finken, A.B. Nair, V.H. Grassian, J. Catal. 191 (2000) 138.
[6] T.N. Obee, S.O. Hay, Environ. Sci. Technol. 31 (1997) 2034.
[7] C. Hagglund, B. Kasemo, L. Osterlund, J. Phys. Chem. B 109 (2005) 10886.
[8] K.L. Miller, C.W. Lee, J.L. Falconer, J.W. Medlin, J. Catal. 275 (2010) 294.
[9] L.F. Liao, W.C. Wu, C.Y. Chen, J.L. Lin, J. Phys. Chem. B 105 (2001) 7678.

[10] S. Sato, K. Ueda, Y. Kawasaki, R. Nakamura, J. Phys. Chem. B 106 (2002) 9054.
[11] D.S. Muggli, J.L. Falconer, J. Catal. 187 (1999) 230.
[12] T. Chen, G.P. Wu, Z.C. Feng, G.S. Hu, W.G. Su, P.L. Ying, C. Li, Chin. J. Catal. 29 (2008) 105.
[13] H. Idriss, A. Miller, E.G. Seebauer, Catal. Today 33 (1997) 215.
[14] K. Takahashi, H.J. Yui, J. Phys. Chem. C 113 (2009) 20322.
[15] J. Peral, X. Domènech, D.F. Ollis, J. Chem. Technol. Biotechnol. 70 (1997) 117.
[16] A. Vittadini, A. Selloni, F.P. Rotzinger, M. Gratzel, J. Phys. Chem. B 104 (2000) 1300.
[17] A. Vittadini, A. Selloni, F.P. Rotzinger, M. Gratzel, Phys. Rev. Lett. 81 (1998) 2954.
[18] X.Q. Gong, A. Selloni, A. Vittadini, J. Phys. Chem. B 110 (2006) 2804.
[19] G. Kresse, J. Furthmuller, Comput. Mater. Sci. 6 (1996) 15.
[20] G. Kresse, J. Hafner, Phys. Rev. B 47 (1993) 558.
[21] D. Vanderbilt, Phys. Rev. B 41 (1990) 7892.
[22] M.A. Szymanski, M.J. Gillan, Surf. Sci. 367 (1996) 135.
[23] F.P. Rotzinger, J.M. Kesselman-Truttmann, S.J. Hug, V. Shklover, M. Gratzel, J. Phys. Chem. B 108 (2004) 5004.
[24] J.A. Anderson, B.W. Hopkins, J.L. Chapman, G.S. Tschumper, J. Mol. Struct. 771 (2006) 65.
[25] M.R. Johnson, H.P. Trommsdorff, Chem. Phys. 355 (2009) 118.
[26] M. Plazanet, N. Fukushima, M.R. Johnson, A.J. Horsewill, H.P. Trommsdorff, J. Chem. Phys. (2001) 3241.
[27] G.B. Deacon, F. Huber, R.J. Phillips, Inorg. Chim. Acta 104 (1985) 41.
[28] G.B. Deacon, R.J. Phillips, Coord. Chem. Rev. 33 (1980) 227.
[29] G.S. Herman, Z. Dohnalek, N. Ruzycki, U. Diebold, J. Phys. Chem. B 107 (2003) 2788.
[30] Y.B. He, A. Tilocca, O. Dulub, A. Selloni, U. Diebold, Nat. Mater. 8 (2009) 585.
[31] W.K. Li, X.Q. Gong, G. Lu, A. Selloni, J. Phys. Chem. C 112 (2008) 6594.
[32] D.S. Muggli, M.J. Backes, J. Catal. 209 (2002) 105.
[33] M.J. Backes, A.C. Lukaski, D.S. Muggli, Appl. Catal. B 61 (2005) 21.
[34] M.A. Henderson, Langmuir 21 (2005) 3443.
[35] P.R. McGill, H. Idriss, Surf. Sci. 602 (2008) 3688.
[36] M. Bowker, P. Stone, R. Bennett, N. Perkins, Surf. Sci. 511 (2002) 435.
[37] J. Araña, C. Garriga i Cabo, J.M. Doña-Rodríguez, O. González-Díaz, J.A. Herrera-Melián, J. Pérez-Peña, Appl. Surf. Sci. 239 (2004) 60.
[38] M.F.J. Dijkstra, H.J. Panneman, J.G.M. Winkelman, J.J. Kelly, A.A.C.M. Beenackers, Chem. Eng. Sci. 57 (2002) 4895.
[39] M.A. Henderson, J.M. White, H. Uetsuka, H. Onishi, J. Catal. 238 (2006) 153.
[40] W.C. Wu, C.C. Chuang, J.L. Lin, J. Phys. Chem. B 104 (2000) 8719.